Journal of Food Composition and Analysis 148 (2025) 108571

Contents lists available at ScienceDirect

Journal of Food Composition and Analysis

journal homepage: www.elsevier.com/locate/jfca

Shining light on olive trees: Hydroxytyrosol screening in leaves by fluorescence spectroscopy

Tommaso Ugolini [d], Barbara Adinolfi [a,*], Andrea Azelio Mencaglia [a], Graziano Sani [b], Laura Bonora [b], Nadia Mulinacci [c], Lorenzo Cecchi [d,*], Irene Digiglio [c], Anna Grazia Mignani [a,*], Leonardo Ciaccheri [a]

[a] National Research Council of Italy (CNR), Institute of Applied Physics (IFAC), Via Madonna del Piano 10, 50019 Sesto Fiorentino, Florence, Italy
[b] National Research Council of Italy (CNR), Institute of Bio Economy (IBE), 50019 Sesto Fiorentino, Florence, Italy
[c] Department of NEUROFARBA and Multidisciplinary Centre of Research on Food Sciences (M.C.R.F.S.- Ce.R.A), University of Florence, Via Ugo Schiff 6, 50019 Sesto Fiorentino, Florence, Italy
[d] Department of Agriculture, Food, Environment and Forestry (DAGRI), University of Florence, Piazzale Delle Cascine 16, 50144 Florence, Italy

ARTICLE INFO

Keywords:
Fluorescence
Chemometrics
Hydroxytyrosol
Olive leaves
Virgin olive oil by-products

ABSTRACT

An innovative, non-destructive, and rapid method was introduced to quantify hydroxytyrosol content in olive leaves by means of advanced photonic technologies and chemometrics. At the heart of this approach is a custom-made, pocket-sized fluorometer with LED excitation at 375 nm and a miniaturized spectrometer for emission detection in the visible range, designed to measure intact olive leaves with ease and precision. Four Italian olive cultivars, namely Frantoio, Leccino, Leccio del Corno, and Moraiolo, were studied, with nine leaf samplings conducted over the 2022–2024 period. Simultaneously, hydroxytyrosol concentration was measured using HPLC-DAD-MS on the same samples to establish the reference data. Chemometric analysis was applied to the spectroscopic and HPLC-DAD-MS results. The Orthogonal Partial Least Squares (OPLS) regression method was successfully used to build a predictive model to quantify hydroxytyrosol concentrations ranging from 200 to 7000 mg/kg. The model achieved very good regression coefficients of 0.9 for calibration and 0.83 for cross-validation, with root mean square errors of 600 mg/kg and 720 mg/kg, respectively. This non-destructive method, combined with the portability of the pocket-sized fluorometer, is an innovation for high-throughput screening of olive leaves. It offers significant potential for evaluating olive leaves before their use in tea production or as raw material for dietary supplements, making it highly appealing for both the agriculture and health industries.

1. Introduction

Olive trees *(Olea europaea* L.) are invaluable assets to economies, cultures, environments, and health sectors, significantly enhancing the regions where they are cultivated. Primarily grown for their olives, the main product, these trees also produce several valuable by-products utilized across various industries and applications (Selim et al., 2022; Doménech et al., 2021; El Asri et al., 2022; Delgado et al., 2023; Valenti et al., 2025). Just think that in the two months of olive harvesting for oil production, approximately 1 ton of olives produce approximately 1–2 tons of liquid waste product called Olive Mill Wastewater (OMWW) and 800 kg of solid waste called olive pomace (OP) (El Asri et al., 2022). The various waste products represent an important resource for applications in agriculture, bioenergy (El Asri et al., 2022; Delgado et al., 2023) and for health. Among these by-products, olive tree leaves are the most unavoidable and abundant, yielding approximately 25 kg per tree during pruning (Palmeri et al., 2022; Espeso et al., 2021; Markhali et al., 2020; Wasim, Bergonzi, 2025). Turning olive leaves from a costly by-product into a valuable source of antioxidants is a challenging opportunity. This transformation not only offers economic and environmental advantages but also enhances health and stimulates innovation (Ronca et al., 2024; Mansour et al., 2023; Rocha-Pimienta et al., 2020; Borjan et al., 2020; Kiritsakis et al., 2017; Najla et al., 2022; Vasarri et al., 2024).

Hydroxytyrosol (HT) is a natural phenolic compound found in extra virgin olive oil and olive leaves. It has attracted significant interest due

* Corresponding authors.
E-mail addresses: b.adinolfi@ifac.cnr.it (B. Adinolfi), lo.cecchi@unifi.it (L. Cecchi), a.g.mignani@ifac.cnr.it (A.G. Mignani).

https://doi.org/10.1016/j.jfca.2025.108571
Received 10 January 2025; Received in revised form 30 October 2025; Accepted 5 November 2025
Available online 7 November 2025

to its beneficial properties for human health, as demonstrated by numerous studies (Wang et al., 2025). Several *in vitro* and *in vivo* studies described in the literature reported that HT has numerous pharmacological properties potentially useful for improving human health (Bertelli et al., 2020; Cornali et al., 2025). The most important ones are surely its antioxidant and anti-inflammatory properties (Aeschbach et al., 1994; Calahorra et al., 2018; Pojero et al., 2022; Fuccelli et al., 2018; Silva et al., 2015; Gu et al., 2025; Lillis et al., 2025; Tang et al., 2025; Prevete et al., 2025; Salvo, Tuttolomondo, 2025), which are closely correlated with the cytotoxic and antiproliferative properties demonstrated on various human tumor cell lines (Bernini et al., 2015; Granados-Principal et al., 2011; Sánchez-Quesada et al., 2022; Gonçalves et al., 2024; Toteda et al., 2017; Melo Ferreira et al., 2025; Salvo, Tuttolomondo, 2025). Additionally, cardioprotective properties have been demonstrated, showing HT as able to prevent and reduce the risk of the onset of cardiovascular diseases and the formation of atherosclerotic plaques (Noguera-Navarro et al., 2023; D'Angelo et al., 2020; X. Zhang et al., 2020; Wang et al., 2025; Salvo, Tuttolomondo, 2025). The anti-atherosclerotic action of HT can be traced back to the antioxidant action of this phenol, which leads to the stimulation of the synthesis of antioxidant enzymes, an event that also limits the lipid peroxidation of LDL cholesterol, a hallmark of atherosclerosis (Hou et al., 2025). Also, the lipolytic action of HT on human primary visceral adipocytes has been demonstrated (Stefanon, Colitti, 2016). Other properties attributed to HT are the neuroprotective, antibacterial and antiviral ones (González-Correa et al., 2008; Prevete et al., 2025; Barrera-Chamorro et al., 2025; Ben Hassena et al., 2025). The latter was described by *in vitro* and clinical studies, showing that treatment with a nasal HT spray increased the body's defenses against SARS-CoV-2 infections and reduced the synthesis of viral particles (Paolacci et al., 2021).

As awareness of HT health benefits continues to grow, the demand for HT-based dietary supplements is expected to rise. These supplements are often produced as tablets from crushed, purified olive leaves, ensuring a consistent and precise dosage of HT. This process maximizes the value of olive tree byproducts and offers a natural plant-based supplement option. Tablets make it easy for individuals to incorporate this potent antioxidant into their daily routines, providing a reliable and measurable dose for better health outcomes. Their convenience and ease of consumption enhance adherence to supplementation, seamlessly integrating into everyday habits.

In addition to supplements, crushed olive leaves are increasingly being used to make tea bags, providing a natural, flavorful alternative to traditional herbal teas. By crushing the leaves, their beneficial compounds are more easily released during steeping, extracting flavors and active compounds, and offering a convenient way to enjoy the HT powerful antioxidant property.

Aiming to assess the suitability of olive leaves for producing HT-based tablets and tea bags, this paper presents an innovative, rapid and non-destructive method for quantifying HT. This method offers the potential for high-throughput screening of olive leaves prior to processing. A low-cost, custom-made, pocket-sized fluorometer was used to measure the fluorescence spectra of selected leaves. Simultaneously, HT quantitation was achieved by HPLC-DAD-MS to have reference data. The fluorescence and HPLC-DAD-MS data were processed using chemometric techniques to develop a predictive model for HT quantitation.

2. Material and methods

2.1. Chemicals

Ultrapure water was produced using the Milli-Q-system (Millipore SA, Molsheim, France). Formic acid, HPLC-grade methanol and acetonitrile as well as analytical-grade methanol and ethanol, and a commercial standard of Tyrosol were purchased from Merck (Darmstadt, Germany). .

2.2. Experimental plan

Olive leaf samples were collected from the rural area surrounding Florence (Tuscany, Italy). To ensure a comprehensive study of the leaves' antioxidant potential, four widely cultivated olive varieties (Frantoio, Leccio del Corno, Moraiolo, and Leccino) were selected. These cultivars are well-known for their distinct quality and contributions to extra virgin olive oil production.

Leaf sampling was conducted over a two-year span, from April 2022 to February 2024, to account for seasonal variations that influence the phytochemical profile of plant materials. A total of nine samplings were carried out, capturing data across spring, summer, autumn, and winter. Details of sampling are given in Table 1. To minimize variability due to environmental factors, all samples were collected from the same experimental olive orchard and, for each sampling period, on the same day.

For each cultivar (4) and sampling time (9), three separate batches of fresh leaves were independently dried at 80 °C in an oven to constant weight and then extracted for HPLC analysis purposes, for a total of 108 samples analyzed; the three batches were treated as biological replicates of the same sample. Quantitative values were expressed as the mean of triplicate measurements. Simultaneously, for each cultivar (4) and sampling time (9), five separate batches of fresh leaves were spectroscopically analyzed with the custom-made spectrofluorometer, for a total of 180 samples analyzed. Such batches were treated as replicates of the same sample, which was characterized by the mean spectrum of the five replicates.

The subsequent chemometric analysis was carried out using the mean spectra and the mean HPLC data. Therefore, the dataset consisted of 36 observations (4 cultivar × 9 time points).

2.3. Quantitative analysis of olive leaves by HPLC-DAD-MS

HT was analyzed using HPLC-DAD-MS. Dried leaves were pulverized and homogenized with an IKA M 20 Universal mill. About 1 g of each leaf powder sample was exactly weighed and extracted twice with 30 ml of EtOH:H_2O 80:20, using an IKA T 25 digital Ultraturrax and an ultrasonic bath. After centrifugation at 5000 rpm at 0 °C for 10 min, the extracts were defatted twice with hexane (30 ml), and then the solvent was vacuum evaporated. The dried extract was reconstituted in 5 ml of MeOH:H_2O 50:50, then centrifuged at 14000 rpm for 5 min. Two μl were injected for HPLC analyses.

For quantitative analyses, a modular Agilent 1100 L (Agilent Technology, Palo Alto, CA, USA) equipped with autosampler and photodiode detector (DAD) was employed. The stationary phase was a Poroshell 120, EC-C18 column (150 mm × 3.0 mm 2.7 μm particle dimension; Agilent, Palo Alto, USA). HPLC-grade acetonitrile (A) and ultrapure water acidified with 0.1 % formic acid (B) were used as mobile phase. A linear multistep gradient was employed at a constant flow rate of 0.4 ml/min, as follows: solvent B changed from 95 % to 60 % in 40 min, stayed at 60 % for 5 min, changed from 60 % to 0 % in 5 min, remained at 0 % for 3 min and finally returned to 95 % in 2 min, for a total analysis time of 55 min. The system was equilibrated for 10 min before injection. UV-

Table 1
The collected olive leaf samples, with month and season of each epoch.

Sampling epoch	Sampling month	Sampling season
1	Apr−22	Spring
2	Jul−22	Summer
3	Oct−22	Autumn
4	Feb−23	Winter
5	Apr−23	Spring
6	Jul−23	Summer
7	Aug−23	Summer
8	Nov−23	Autumn
9	Feb−24	Winter

Visible spectra were acquired between 200 and 550 nm, and chromatograms were recorded at 210, 220, 240, 380 and 350 nm. HT was quantitated using an external calibration curve of tyrosol (y = 1462.2x; $R^2 = 1$) prepared with the following solutions: A) 0.101 mg/ml in EtOH:H_2O^+ (H_2O^+ = ultrapure water acidified to pH = 3.2 with formic acid) 70:30. B) 0.0101 mg/ml in EtOH:H_2O^+ 70:30; λ = 280 nm. For the characterization of the extracts, a 1260 Infinity II LC system, coupled to a DAD and a Mass Spectrometry Detector (InfinityLab LC/MSD) with API/ESI interface (Agilent Technology, Palo Alto, CA, USA) was used under the same chromatographic conditions described above.

2.4. Pocket-sized LED-based fluorometer and leaf measurements

Figure S1 shows a rendering of the fluorometer used in this study (Mencaglia et al., 2023). The optical head for fluorescence excitation houses an array of twelve circularly arranged LEDs emitting at 375 nm. Given the need to keep the fluorometer compact and pocket-sized, a 3 mm-cased LED is the most suitable choice. Among the commercially available options, the 375 nm LED offers the highest emission intensity and the narrowest beam angle, making it the optimal solution for this application (Roithner LaserTechnik GmbH, XSL-375–3E: AlGaN LED chip die mounted on a lead frame hermetically sealed with a clear UV resin lens; radiated power 14 mW at 20 mA, halfwidth = 15 nm). These LEDs are set at a 45° angle in relation to the axis of detection, situated at the center of the circle. This opto-geometric arrangement minimizes the influence of any surface texture or roughness effects. LEDs are powered by a commercially available electronic controller (PhidgetsLED1031, Phidgets Inc. Calgary, Canada), which interfaces via USB connection with a laptop PC. The optical head is butt-coupled to a cylinder that accommodates the detector. Specifically, it is an Ocean Optics ST VIS Microspectrometer from Ocean Optics (Orlando, FL, USA) that operates in the 350–810 nm range, having a spectroscopic resolution of 1.5 nm. The detector is also connected to the USB port of the laptop.

Given that the LED spectra extend in the visible range, a short-pass filter is positioned between the optical head and the measurement spot to avoid illumination at wavelengths longer than 400 nm. This filter is designed with a minute hole aligned with the spectrometer's input slit, thus facilitating the capture of backscattered fluorescence light intensity only at wavelengths longer than 400 nm.

The hardware modules are controlled by means of a suitably developed LabVIEW® software interface (National Instruments Corp., Austin TX, USA). This interface operates LEDs, spectrometer and detector acquisition, and shows the measured spectra in a visual form on the display of the PC, while the data can be saved in an Excel file.

The fluorometer is designed to be lightweight and easily manageable. The optical head housing the LEDs, the cylinder containing the spectrometer butt-coupled to the optical head, and the casing of the electronic board were all fabricated using 3D printing technology (KLONER3D®, Firenze, Italy), employing a polylactic acid wire as the material. This optical head measures 60 mm in diameter and 74 mm in height, with a weight of 170 g, making it particularly suitable for portable or handheld applications, as well as for integration into larger optical or sensing systems where space and weight constraints are critical. Despite its small form factor, the optical head maintains high mechanical stability and optical precision, ensuring reliable performance in both laboratory and field environments.

Figure S2 and S3 show the fluorometer with the power supply and the optical head, respectively. Figure S4 shows the setup during leaf measurements, carried out on fresh leaves.

2.5. Chemometric processing of spectroscopic and HPLC data for quantifying hydroxytyrosol

Quantitative HPLC-DAD-MS data were subjected to one-way ANOVA. Significant statistical differences among sampling epochs ($p < 0.05$) were assessed by Tukey's HSD test. ANOVA and Tukey's test were performed using software R version 4.3.1 (The R Foundation for Statistical Computing).

The concentration of HT was predicted from fluorescence data by means of the Orthogonal Partial Least Squares (OPLS) regression and compared with HPLC data. The SIMCA17® software was used for data processing and visualization. OPLS is a technique particularly suitable for predicting quantitative variables such as the concentration of an analyte in a multicomponent mixture (Vajargah et al., 2012; Bylesjö et al., 2006). OPLS is a development of PLS regression method. Unlike PLS, which produces several predicting components in decreasing order of importance, OPLS produces one predicting component and several orthogonal components that model the interfering factors influencing the spectrum. This allows for a more straightforward interpretation of the model. Model performance was assessed by:

- Coefficients of determination, R^2 and Q^2, which are the ratios of modelled variance over total variance of target variable for calibration and cross-validation, respectively. R^2 is a measure of model fitting, while Q^2 provides a measure of its prediction ability. The fit is good when R^2 and Q^2 are similar and close to 1.
- Root Mean Square Error of Calibration (RMSEC), and Root Mean Square Error of Cross-Validation (RMSECV), which estimate the prediction errors in calibration and cross-validation, respectively. The closeness of RMSEC and RMSECV provides an estimation of robustness of the predictive model.

In practice, the OPLS method allows predicting the concentration of an analyte in the n^{th} sample by means of fluorescence spectroscopy and Eq. 1:

$$\widehat{y_n} = \langle y \rangle + \sum_{m=1}^{M} r_m \left(x_{n\ m} - \langle x \rangle_m \right) \quad (1)$$

where:

- M = number of spectral channels (wavelengths).
- r_m = regression coefficient corresponding to m^{th} wavelength.
- $x_{n\ m}$ = value of the fluorescence spectrum of n^{th} sample at m^{th} wavelength.
- $\langle x_m \rangle$ = mean value of fluorescence spectrum at m^{th} wavelength, for the calibration set.
- $\langle y \rangle$ = mean value of target variable for the calibration set.

The OPLS predictive model was developed and optimized using 9-fold cross-validation, because the limited size of data set available did not allow dividing conveniently the entire dataset into a calibration and a validation set. However, in order to make cross-validation more challenging, a scheme was chosen that left out a whole sampling at a time. In such a way, each sampling was predicted by a model calibrated with independently sampled leaves.

3. Results and discussion

3.1. HPLC data of hydroxytyrosol

Fig. 1 illustrates concentrations of HT in olive leaves collected from different cultivars across various sampling periods. Quantitative data from HPLC-DAD analysis revealed a broad range of HT levels, from 200 mg/kg to 7000 mg/kg on a dry weight basis. HT concentrations varied significantly depending on season, with consistently lower values observed from summer to autumn (Blasi et al., 2016; Losada-Echeberría et al., 2022; Obied et al., 2008; Talhaoui et al., 2015; Palmeri et al., 2022). However, all four olive cultivars (Frantoio, Leccio del Corno, Moraiolo, and Leccino) exhibited similar trends in HT content throughout the year. The near-independence of HT levels from the specific cultivar is noteworthy, as it suggests the feasibility of developing predictive models for HT concentration that are broadly applicable,

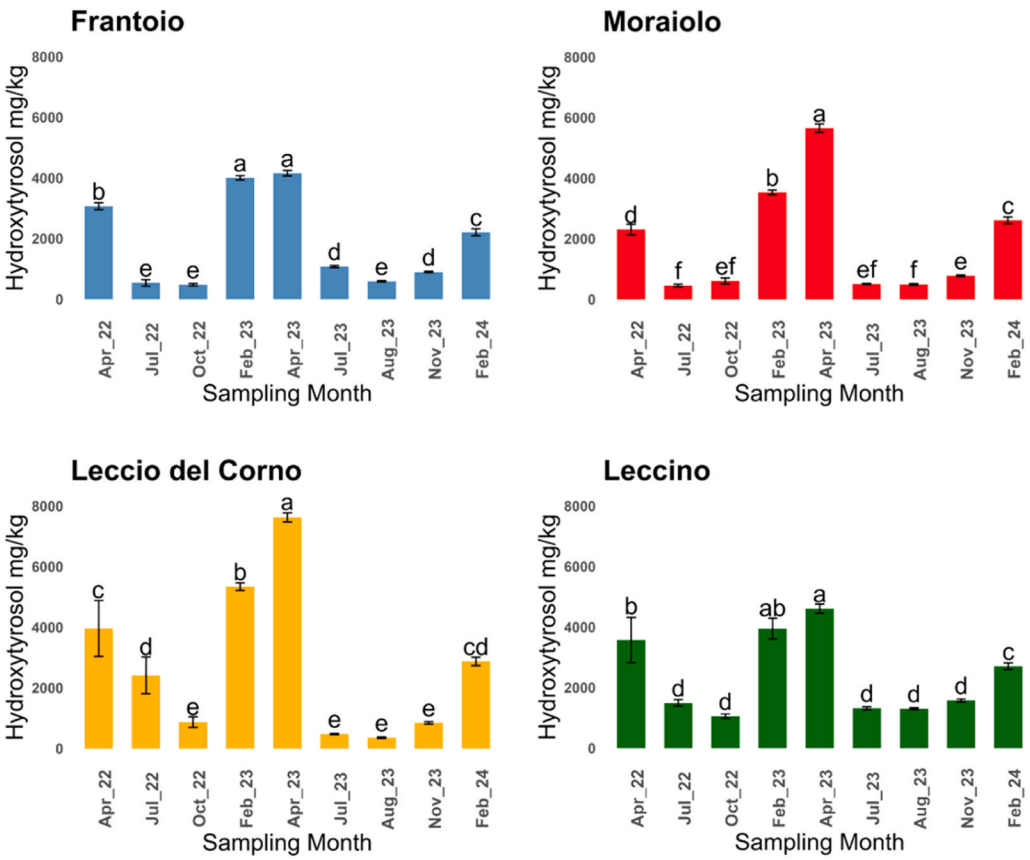

Fig. 1. Hydroxytyrosol content (mg/kg dried leaves) from HPLC-DAD analysis in samples from different sampling times, grouped according to the cultivars. Solid bars represent means of biological triplicates, while error bars represent standard deviations. Groups of means marked with different letters are significantly different at the 0.05 level according to Tukey's HSD test.

regardless of whether a single or multiple cultivar are grown within a given orchard. Among the selected cultivars, Leccio del Corno exhibited the highest HT levels, especially in the spring, indicating the importance of seasonal timing to maximize antioxidant yield from olive leaves. This data suggests that spring might be the optimal period for harvesting olive leaves to achieve optimal HT levels, particularly from the Leccio del Corno cultivar. These results underscore how both cultivar and seasonal changes influence HT levels in olive leaves, ensuring a well-rounded understanding for optimizing their use in nutraceutical and food applications.

3.2. *Fluorescence spectra of olive leaves*

Leaves collected from each cultivar and sampling period were divided into two groups. Approximately four hours after sampling, sixty leaves were scanned for each sample, using the custom-made fluorometer in overlapping pairs to increase sample thickness. The integration time for each scan was set at 1000 ms, and each scan was the average of three readouts. In total, 30 scans were conducted, which were then averaged to obtain the mean spectrum for each cultivar and sampling epoch. The remaining leaves were used to measure HT content via HPLC-DAD, which served as a reference for HT quantitation.

The spectroscopic range of 425–650 nm was selected for analysis. Data below 425 nm were discarded due to interference from residual intensity caused by LED excitation, and data above 650 nm were excluded as they were dominated by chlorophyll fluorescence (Pedrós et al., 2008).

Fig. 2 displays the fluorescence spectra of the olive leaves within the selected wavelength band, color-coded according to the sampling seasons. These spectra were derived from the measured data after applying

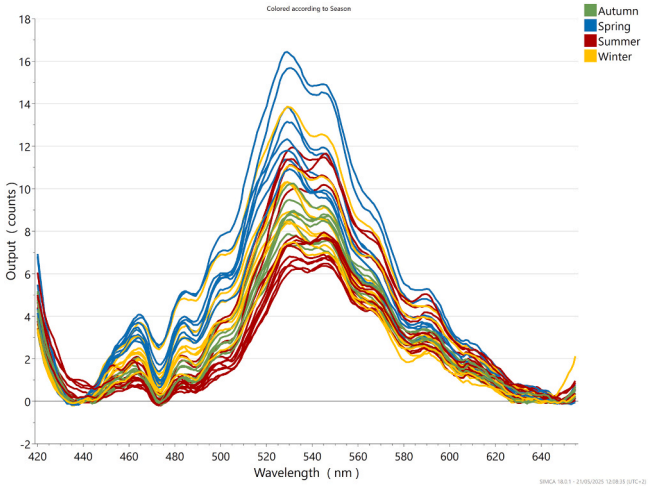

Fig. 2. Fluorescence spectra of olive tree leaves colored according to sampling time.

baseline correction using the Antisymmetric Least Squares algorithm (AsLS-C) (F. Zhang et al., 2020). The smoothing factor was set at 10^5 to ensure a smooth baseline, while the asymmetry factor was set at 0.01, providing greater sensitivity to baseline asymmetry.

These spectra are consistent with the literature findings, which attribute blue-green fluorescence in leaves to various phenolic compounds bound to the epidermal cell walls. The identity of such phenols is still unclear, and several compounds in addition to HT contribute to the

fluorescence (Schweiger et al., 1996). As already noted in the HPLC data, these fluorescence spectra showed seasonal variation but no significant dependence on cultivar.

3.3. Quantitation of hydroxytyrosol

The detailed spectral analysis, combined with HPLC data, enabled precise quantitation of HT content across cultivars and seasons. The optimal regression model was achieved using 1 predictive component and 3 orthogonal components for modeling the spectral variance not related to HT. The regression model explains 99.3 % of total spectra variance, but only 48.5 % is used for prediction, while the remaining 50.8 % is used for modelling interfering factors. Fig. 3 shows the loadings of predicting component, p[1], compared to those of the 1st orthogonal component, po[1], which accounts for 42.8 % of variance. It is interesting to know that the informative part of the spectrum does not coincide with the main peak of fluorescence band at 530–550 nm, which is explained by the orthogonal component, but it is shifted towards shorter wavelengths. This means that multiple substances contribute to fluorescence emission in the blue-green band.

Table 2 provides a detailed summary of the statistical analysis results. Despite the sensible interference, the method achieved a satisfactory performance, with a coefficient of determination of 0.902 for calibration and 0.835 for cross-validation. The calibration error was 600 mg/kg, while cross-validation error was 720 mg/kg, which corresponds to 32 % of the mean HT content of dataset (2240 mg/kg).

For a clearer understanding of these outcomes, Fig. 4 presents the regression curves, with the calibration curve (Fig. 4A) and the cross-validation curve (Fig. 4B). These visual representations highlight the close agreement between predicted and actual HT concentrations, confirming the effectiveness of the model in both the calibration and validation phases.

These results show that the proposed approach allows monitoring HT in fresh olive leaves to be used for dietary and nutritional supplements.

4. Conclusions

An innovative method for real-time quantitation of HT in olive tree leaves was developed using a low-cost, pocket-sized fluorometer, combined with chemometric analysis of spectroscopic data. Leaves from four different cultivars were collected, with samples taken across various seasons from 2022 to 2024. By applying OPLS regression to the fluorescence spectra and using HPLC data as a reference, good prediction of HT concentration was achieved. The regression coefficients for calibration and cross-validation were 0.9 and 0.83, respectively, with root mean square errors of 600 mg/kg for calibration and 720 mg/kg for cross-validation. Future research, including external validation, is required to confirm these good results. Remarkably, the results showed that HT levels were consistent across cultivars, while they varied significantly depending on the season.

This paper marks the first successful use of fluorescence spectroscopy via a pocket-sized fluorometer for screening HT concentrations in fresh olive leaves. The method offers a fast, non-destructive solution for determining HT levels without the need for complex laboratory equipment. Moving forward, the next aim is to further enhance this device by integrating a standalone data processing unit and display, eliminating the need for a laptop. Our ultimate vision is to transform this fluorometer into a high-throughput analytical tool capable of efficiently identifying olive leaves with the highest HT concentrations, all without the

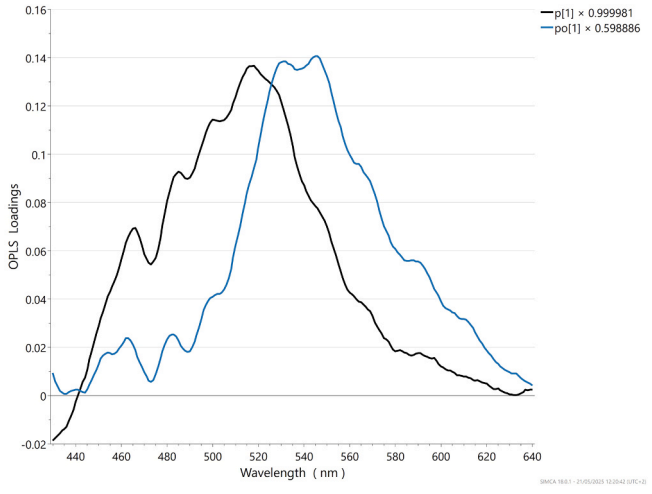

Fig. 3. OPLS loading of predicting component, p[1], and 1st orthogonal component, po[1].

Table 2
Statistical parameters of OPLS regression.

OPLS Regression Statistics		
LV	Number of OPLS components: predicting + orthogonal	1 + 3
R^2	Determination coefficient of calibration	0.9
Q^2	Determination coefficient of cross-validation	0.84
RMSEC (mg/Kg)	Root Mean Square Error of Calibration	600
RMSECV (mg/Kg)	Root Mean Square Error of Cross-Validation	720

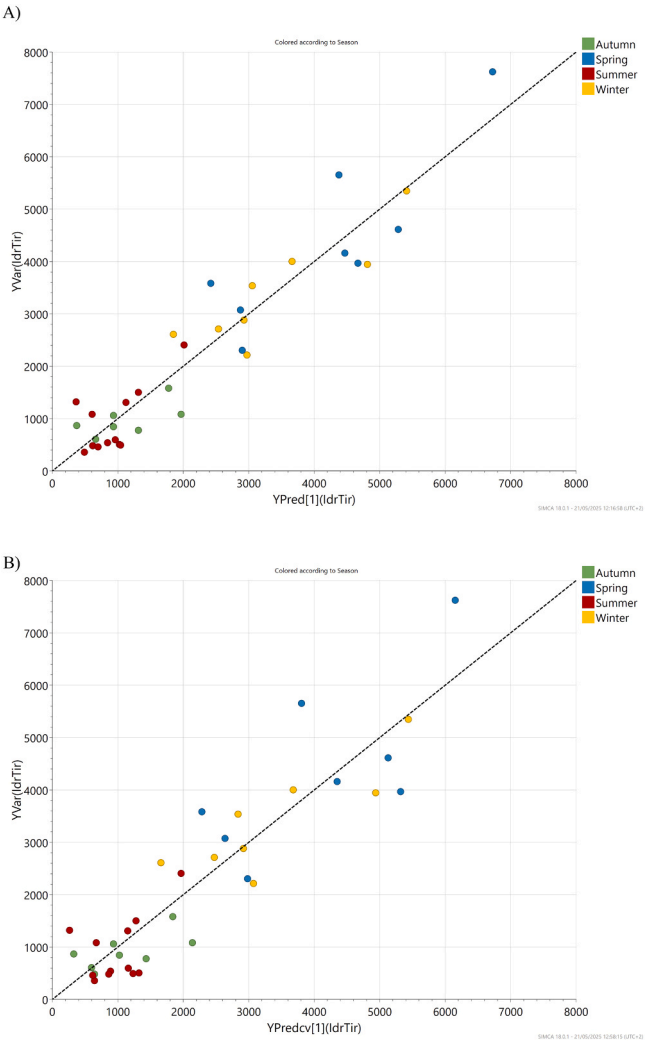

Fig. 4. OPLS regression curve for the calibration (A) and cross-validation (B).

need for chemicals or specialized personnel.

This breakthrough has the potential to improve the production of high-quality dietary supplements and other olive leaf-derived products, such as tea bags. By enabling real-time, non-destructive quantitation of HT directly from intact leaves, this method streamlines the selection process, ensuring that only the most antioxidant-rich leaves are used for further processing. The ability to assess HT levels quickly and accurately, without expensive equipment or specialized expertise, opens new possibilities for both small-scale producers and large manufacturers. The affordability, simplicity, and scalability of the technique presented make it a game-changing tool that promotes sustainable practices and offers a competitive advantage in the growing market for natural, antioxidant-rich products.

In addition to the demonstrated possibility to rapidly quantify hydroxytyrosol, the strength of proposed approach is its intrinsic versatility: with appropriate calibration, it could be extended to quantify other key bioactive compounds in olive leaves, such as Oleuropein. This opens the door to broader applications of the technique, including comprehensive profiling of antioxidant content in olive-based products, which could benefit both producers and consumers seeking high-quality, natural health supplements.

Author statement

All persons who meet authorship criteria are listed as authors, and all authors certify that they have participated sufficiently in the work to take public responsibility for the content, including participation in the concept, design, analysis, writing, or revision of the manuscript.

CRediT authorship contribution statement

Tommaso Ugolini: Writing – review & editing, Writing – original draft, Methodology, Investigation, Formal analysis. **Barbara Adinolfi**: Writing – review & editing, Methodology, Investigation. **Andrea Azelio Mencaglia**: Writing – review & editing, Resources, Methodology. **Graziano Sani**: Writing – review & editing, Methodology, Investigation, Conceptualization. **Laura Bonora**: Writing – review & editing, Investigation. **Nadia Mulinacci**: Writing – review & editing, Resources, Methodology. **Lorenzo Cecchi**: Writing – review & editing, Methodology, Investigation. **Irene Digiglio**: Investigation, Formal analysis. **Anna Grazia Mignani**: Writing – review & editing, Writing – original draft, Resources, Methodology, Investigation. **Leonardo Ciaccheri**: Writing – review & editing, Writing – original draft, Software, Resources, Methodology, Investigation, Formal analysis, Conceptualization.

Ethical statement

This study does not involve any animal or human study.

Declaration of Competing Interest

The authors declare that they have no known competing financial interests or personal relationships that could have appeared to influence the work reported in this paper.

Acknowledgments

The “Agrosensing” CNR-DIITET FOE 2020 project is acknowledged for partial financial support.

Appendix A. Supporting information

Supplementary data associated with this article can be found in the online version at doi:10.1016/j.jfca.2025.108571.

Data availability

Data will be made available on request.

References

Aeschbach, R., Löliger, J., Scott, B.C., Murcia, M.A., Butler, J.J., Halliwell, B., Aruoma, O. I., 1994. Antioxidant actions of thymol, carvacrol, 6-gingerol, zingerone and hydroxytyrosol. Food Chem. Toxicol. 32, 31–36. https://doi.org/10.1016/0278-6915(84)90033-4.

Barrera-Chamorro, L., Fernandez-Prior, A., Claro-Cala, C.M., Del Rio-Vazquez, J.L., Rivero-Pino, F., Montserrat-de la Paz, S., 2025. Unveiling the neuroprotective impact of virgin olive oil ingestion via the microbiota-gut-brain axis. Food Funct. J. 16, 24–39. https://doi.org/10.1039/d4fo04560b.

Ben Hassena, A., Abidi, J., Miled, N., Kulinowski, Ł., Skalicka-Woźniak, K., Bouaziz, M., 2025. New insights into the antibacterial activity of hydroxytyrosol extracted from olive leaves: molecular docking simulations of its antibacterial mechanisms. Chem. Biodivers. 22, e202401714 https://doi/10.1002/cbdv.202401714.

Bernini, R., Gilardini Montani, M.S., Merendino, N., Romani, A., Velotti, F., 2015. Hydroxytyrosol-derived compounds: a basis for the creation of new pharmacological agents for cancer prevention and therapy. J. Med. Chem. 58, 9089–9107. https://doi.org/10.1021/acs.jmedchem.5b00669.

Bertelli, M., Kiani, A.K., Paolacci, S., Manara, E., Kurti, D., Dhuli, K., Bushati, V., Miertus, J., Pangallo, D., Baglivo, M., Beccari, T., Michelini, S., 2020. Hydroxytyrosol: a natural compound with promising pharmacological activities. J. Biotechnol. 309, 29–33. https://doi.org/10.1016/j.jbiotec.2019.12.016.

Blasi, F., Urbani, E., Simonetti, M.S., Chiesi, C., Cossignani, L., 2016. Seasonal variations in antioxidant compounds of *Olea europaea* leaves collected from different Italian cultivars. J. Appl. Bot. Food Qual. 89, 202–207. https://doi.org/10.5073/JABFQ.2016.089.025.

Borjan, D., Leitgeb, M., Knez, Ž., Hrnčič, M.K., 2020. Microbiological and antioxidant activity of phenolic compounds in olive leaf extract. article e5946. Molecules 25. https://doi.org/10.3390/molecules25245946.

Bylesjö, M., Rantalainen, M., Cloarec, O., Nicholson, J.K., Holmes, E., Trygg, J., 2006. OPLS discriminant analysis: combining the strengths of PLS-DA and SIMCA classification. J. Chemom. 20, 341–351. https://doi.org/10.1002/cem.1006.

Calahorra, J., Martínez-Lara, E., Dios, C.D., Siles, E., 2018. Hypoxia modulates the antioxidant effect of hydroxytyrosol in MCF-7 breast cancer cells. PLOS ONE 13, e0203892. https://doi.org/10.1371/journal.pone.0203892.

Cornali, K., Di Lauro, M., Marrone, G., Masci, C., Montalto, G., Giovannelli, A., Schievano, C., Tesauro, M., Pieri, M., Bernardini, S., Noce, A., 2025. The effects of a food supplement, based on Co-Micronized Palmitoylethanolamide (PEA)-Rutin and hydroxytyrosol, in metabolic syndrome patients: preliminary results. article e413. Nutrients 17. https://doi.org/10.3390/nu17030413.

D'Angelo, C., Franceschelli, S., Quiles, J.L., Speranza, L., 2020. Wide biological role of Hydroxytyrosol: possible therapeutic and preventive properties in cardiovascular diseases. Article e1932. Cells 9. https://doi.org/10.3390/cells9091932.

Delgado, A., Chammem, N., Issaoui, M., Ammar, E., 2023. Bioactive Phytochemicals from Olive (*Olea europaea*) Processing By-products. In: Ramadan Hassanien, M.F. (Ed.), Bioactive Phytochemicals from Vegetable Oil and Oilseed Processing By-products. Reference Series in Phytochemistry. Springer, Cham, pp. 197–233. https://doi.org/10.1007/978-3-030-91381-6_10.

Doménech, P., Duque, A., Higueras, I., Fernández, J.L., Manzanares, P., 2021. Analytical characterization of water-soluble constituents in olive-derived by-products. *Article e*1299. Foods 10. https://doi.org/10.3390/foods10061299.

El Asri, O., Fadlaoui, S., Ramdani, M., 2022. Anaerobic digestion technology of solid and liquid forms of olive wastes in the mediterranean region. In: Ramadan, In.M.F., Farag, M.A. (Eds.), Mediterranean Fruits Bio-wastes. Springer, Cham, pp. 67–89. ⟨https://link.springer.com/chapter/10.1007/978-3-030-84436-3_4⟩.

Espeso, J., Isaza, A., Lee, J.Y., Sörensen, P.M., Jurado, P., Avena-Bustillos, R., de, J., Olaizola, M., Arboleya, J.C., 2021. Olive leaf waste management. Front. Sustain. Food Syst. 5. https://doi.org/10.3389/fsufs.2021.660582.

Fuccelli, R., Fabiani, R., Rosignoli, P., 2018. Hydroxytyrosol exerts anti-inflammatory and anti-oxidant activities in a mouse model of systemic inflammation. Molecules 23. https://doi.org/10.3390/molecules23123212.

Gonçalves, M., Aiello, A., Rodríguez-Pérez, M., Accardi, G., Burgos-Ramos, E., Silva, P., 2024. Olive oil components as novel antioxidants in neuroblastoma treatment: exploring the therapeutic potential of Oleuropein and Hydroxytyrosol. Article e818. Nutrients 16. https://doi.org/10.3390/nu16060818.

González-Correa, J.A., Navas, M.D., Lopez-Villodres, J.A., Trujillo, M., Espartero, J.L., De La Cruz, J.P., 2008. Neuroprotective effect of Hydroxytyrosol and Hydroxytyrosol acetate in rat brain slices subjected to hypoxia-reoxygenation. Neurosci. Lett. 446, 143–146. https://doi.org/10.1016/j.neulet.2008.09.022.

Granados-Principal, S., Quiles, J.L., Ramirez-Tortosa, C., Camacho-Corencia, P., Sanchez-Rovira, P., Vera-Ramirez, L., Ramirez-Tortosa, M.C., 2011. Hydroxytyrosol inhibits growth and cell proliferation and promotes high expression of sfrp4 in rat mammary tumours. Mol. Nutr. Food Res. 55, S117–S126. https://doi.org/10.1002/mnfr.201000220.

Gu, L., Chi, M., Wang, Z., Fu, Y., Li, N., Niu, Y., Yu, B., Lin, J., Li, C., Zhao, G., 2025. Hydroxytyrosol downregulates inflammatory responses via Nrf2/HO-1 axis during fungal keratitis and exerts antifungal effects. Article e114202. Int. Immunopharmacol. 149. https://doi.org/10.1016/j.intimp.2025.114202.

Hou, X.X., Wang, S., Ma, X.X., Wen, Y., Li, Z.J., Liu, X.Y., Zhang, X., Zhang, Y., Qin, X.Y., 2025. Design, synthesis, and biological evaluation of novel hydroxytyrosol

derivatives as protectors for vascular endothelium against lipid overload. Drug Des. Dev. Ther. 19, 2433–2452. https://doi.org/10.2147/DDDT.S500670.
Kiritsakis, A., Shahidi, F., Anousakis, C., 2017. Antioxidants of olive oil, olive leaves, and their bioactivity. In: Shahidi, In.F., Kiritsakis, A. (Eds.), Olives and Olive Oil as Functional Foods: Bioactivity, Chemistry and Processing. John Wiley & Sons Ltd, pp. 367–382. https://doi.org/10.1002/9781119135340.ch19.
Lillis, J.B., Willmott, A.G.B., Chichger, H., Roberts, J.D., 2025. The application of olive-derived polyphenols on exercise-induced inflammation: a scoping review. Article e223. Nutrients 17. https://doi.org/10.3390/nu17020223.
Losada-Echeberría, M., Naranjo, G., Malouche, D., Taamalli, A., Barrajón-Catalán, E., Micol, V., 2022. Influence of Drying Temperature and Harvesting Season on Phenolic Content and Antioxidant and Antiproliferative Activities of Olive (Olea europaea) Leaf Extracts. International Journal of Molecular Sciences 24. https://doi.org/10.3390/ijms24010054. Article e54.
Mansour, H.M.M., Zeitoun, A.A., Abd-Rabou, H.S., El Enshasy, H.A., Dailin, D.J., Zeitoun, M.A.A., El-Sohaimy, S.A., 2023. Antioxidant and anti-diabetic properties of olive (*Olea europaea*) leaf extracts: *in vitro* and *in vivo* evaluation. Article e1275. Antioxidants 12. https://doi.org/10.3390/antiox12061275.
Markhali, F.S., Teixeira, J.A., Rocha, C.M.R., 2020. Olive tree leaves—a source of valuable active compounds. Article e1177. Processes 8. https://doi.org/10.3390/pr8091177.
Melo Ferreira, D., Oliveira, M.B.P.P., Alves, R.C., 2025. A comprehensive review of the antitumor activity of olive compounds: the case of olive oil, pomace, and leaf extracts, phenolic alcohols, secoiridoids, and triterpenes. Article e237. Antioxidants 14. https://doi.org/10.3390/antiox14020237.
Mencaglia, A.A., Ciaccheri, L., Adinolfi, B., Mignani, A.G., 2023. Live demonstration: a LED-based pocket-size and low-cost fluorometer. IEEE Sens. 2023. https://doi.org/10.1109/SENSORS56945.2023.10325123.
Najla, T., Habibi, M., Ammar, M.H., Abazza, L., Mhamdi, R., 2022. Olive fruit by-products: from waste streams into a promising source of value-added products. In: Ramadan, In.M.F., Farag, M.A. (Eds.), Mediterranean Fruits Bio-wastes. Springer, Cham, pp. 47–66. https://doi.org/10.1007/978-3-030-84436-3_3.
Noguera-Navarro, C., Montoro-García, S., Orenes-Piñero, E., 2023. Hydroxytyrosol: its role in the prevention of cardiovascular diseases (Article). Heliyon 9, e12963. https://doi.org/10.1016/j.heliyon.2023.e12963.
Obied, H.K., Bedgood, D., Mailer, R., Prenzler, P.D., Robards, K., 2008. Impact of cultivar, harvesting time, and seasonal variation on the content of biophenols in olive mill waste. J. Agric. Food Chem. 56, 8851–8858. https://doi.org/10.1021/jf801802k.
Palmeri, R., Siracusa, L., Carrubba, M., Parafati, L., Proetto, I., Pesce, F., Fallico, B., 2022. Olive leaves, a promising byproduct of olive oil industry: assessment of metabolic profiles and antioxidant capacity as a function of cultivar and seasonal change. Article e2007. Agronomy 12. https://doi.org/10.3390/agronomy12092007.
Paolacci, S., Ergoren, M.C., De Forni, D., Manara, E., Poddesu, B., Cugia, G., Dhuli, K., Camilleri, G., Tuncel, G., Kaya Suer, H., Sultanoglu, N., Sayan, M., Dundar, M., Beccari, T., Ceccarini, M.R., Gunsel, I.S., Dautaj, A., Sanlidag, T., Connelly, S.T., Bertelli, M., 2021. *In vitro* and clinical studies on the efficacy of α-cyclodextrin and Hydroxytyrosol against SARS-CoV-2 infection. Eur. Rev. Med. Pharmacol. Sci. 25, 81–89. https://doi.org/10.26355/eurrev_202112_27337.
Pedrós, R., Moya, I., Goulas, Y., Jacquemoud, S., 2008. Chlorophyll fluorescence emission spectrum inside a leaf. Photochem. Photobiol. Sci. 7 (4), 498–502. https://doi.org/10.1039/b719506k.
Pojero, F., Aiello, A., Gervasi, F., Caruso, C., Ligotti, M.E., Calabrò, A., Procopio, A., Candore, G., Accardi, G., Allegra, M., 2022. Effects of Oleuropein and Hydroxytyrosol on inflammatory mediators: consequences on inflammaging. Article e380. Int. J. Mol. Sci. 24. https://doi.org/10.3390/ijms24010380.
Prevete, G., Scipioni, E., Donati, E., Villanova, N., Fochetti, A., Lilla, L., Borocci, S., Bernini, R., Mazzonna, M., 2025. Impact of pharmacokinetic enhancement strategies on the antimicrobial and antioxidant activities of hydroxytyrosol. RSC Adv. 15, 3448–3464. https://doi.org/10.1039/d4ra08205b.
Rocha-Pimienta, J., Martín-Vertedor, D., Ramírez, R., Delgado-Adámez, J., 2020. Pro-/antioxidant and antibacterial activity of olive leaf extracts according to bioavailability of phenolic compounds. Emir. J. Food Agric. 32, 479–487. https://doi.org/10.9755/ejfa.2020.v32.i6.2119.
Ronca, C.L., Marques, S.S., Ritieni, A., Giménez-Martínez, R., Barreiros, L., Segundo, M. A., 2024. Olive oil waste as a source of functional food ingredients: assessing polyphenolic content and antioxidant activity in olive leaves. Article e189. Foods 13. https://doi.org/10.3390/foods13020189.
Salvo, A., Tuttolomondo, A., 2025. The role of olive oil in cardiometabolic risk. Article e190. Metabolites 15. https://doi.org/10.3390/metabo15030190.
Sánchez-Quesada, C., Gutiérrez-Santiago, F., Rodríguez-García, C., Gaforio, J.J., 2022. Synergistic effect of squalene and hydroxytyrosol on highly invasive MDA-MB-231 breast cancer cells. Nutrients 14. https://doi.org/10.3390/nu14020255.
Schweiger, J., Lang, M., Lichtenthaler, H.K., 1996. Differences in fluorescence excitation spectra of leaves between stressed and non-stressed plants. J. Plant Physiol. 148, 536–547. https://doi.org/10.1016/S0176-1617(96)80073-3.
Selim, S., Albqmi, M., Al-Sanea, M.M., Alnusaire, T.S., Almuhayawi, M.S., AbdElgawad, H., Al Jaouni, S.K., Elkelish, A., Hussein, S., Warrad, M., El-Saadony, M.T., 2022. Valorizing the usage of olive leaves, bioactive compounds, biological activities, and food applications: a comprehensive review. Front. Nutr. 9. https://doi.org/10.3389/fnut.2022.1008349. Article e1008349.
Silva, S., Sepodes, B., Rocha, J., Direito, R., Fernandes, A., Brites, D., Freitas, M., Fernandes, E., Bronze, M.R., Figueira, M.E., 2015. Protective effects of hydroxytyrosol-supplemented refined olive oil in animal models of acute inflammation and rheumatoid arthritis. J. Nutr. Biochem. 26, 360–368. https://doi.org/10.1016/j.jnutbio.2014.11.011.
Stefanon, B., Colitti, M., 2016. Original research: hydroxytyrosol, an ingredient of olive oil, reduces triglyceride accumulation and promotes lipolysis in human primary visceral adipocytes during differentiation. Exp. Biol. Med. 241, 1796–1802. https://doi.org/10.1177/1535370216654226.
Talhaoui, N., Gomez-Caravaca, A.M., Roldan, C., Leon, L., De la Rosa, R., Fernandez-Gutierrez, A., Segura-Carretero, A., 2015. Chemometric analysis for the evaluation of phenolic patterns in olive leaves from six cultivars at different growth stages. J. Agric. Food Chem. 63, 1722–1729. https://doi.org/10.1021/jf5058205.
Tang, J., Zhang, M., Wang, J., Zhang, H., Wang, Z., Lei, Z., Wang, C., 2025. Hydroxytyrosol ameliorates colon inflammation: mechanistic insights into anti-inflammatory effects, inhibition of the TLR4/NF-kappaB signaling pathway, gut microbiota modulation, and liver protection. Foods 14. https://doi.org/10.3390/foods14071270.
Toteda, G., Lupinacci, S., Vizza, D., Bonofiglio, R., Perri, E., Bonofiglio, M., Lofaro, D., La Russa, A., Leone, F., Gigliotti, P., Cifarelli, R.A., Perri, A., 2017. High doses of hydroxytyrosol induce apoptosis in papillary and follicular thyroid cancer cells. J. Endocrinol. Investig. 40, 153–162. https://doi.org/10.1007/s40618-016-0537-2.
Vajargah, K.F., Sadeghi-Bazargani, H., Mehdizadeh-Esfanjani, R., Savadi-Oskouei, D., Farhoudi, M., 2012. OPLS statistical model versus linear regression to assess sonographic predictors of stroke prognosis. Neuropsychiatr. Dis. Treat. 8, 387–392. https://doi.org/10.2147/NDT.S33991.
Valenti, B., Scicutella, F., Viti, C., Daghio, M., Mannelli, F., Gigante, D., Buccioni, A., Bolletta, V., Morbidini, L., Turini, L., Natalello, A., Servili, M., Selvaggini, R., Pauselli, M., 2025. Olive tree leaves in dairy sheep diet: effects on rumen metabolism, microbiota composition and milk quality. Animal 19. https://doi.org/10.1016/j.animal.2025.101435. Article e101435.
Vasarri, M., Bergonzi, M.C., Ivanova Stojcheva, E., Bilia, A.R., Degl'Innocenti, D., 2024. *Olea europaea* L. leaves as a source of anti-glycation compounds. Molecules 29. https://doi.org/10.3390/molecules29184368. Article e4368.
Wang, W., Du, L., Wei, Q., Lu, M., Xu, D., Li, Y., 2025. Synthesis and health effects of phenolic compounds: a focus on tyrosol, hydroxytyrosol, and 3,4-dihydroxyacetophenone. Antioxidants 14. https://doi.org/10.3390/antiox14040476. Article e476.
Wasim, M., Bergonzi, M.C., 2025. From waste to value: solubility and dissolution enhancement of bioactive extracts from olive leaves using poloxamers. Molecules 30. https://doi.org/10.3390/molecules30040928.
Zhang, X., Qin, Y., Wan, X., Liu, H., Iv, C., Ruan, W., Lu, L., He, L., Guo, X., 2020. Hydroxytyrosol plays antiatherosclerotic effects through regulating lipid metabolism via inhibiting the p38 signal pathway. BioMed. Res. Int. 2020. https://doi.org/10.1155/2020/5036572. Article e5036572.
Zhang, F., Tang, X., Tong, A., Wang, B., Wang, J., 2020. An automatic baseline correction method based on the penalized least squares method. Sensors 20. https://doi.org/10.3390/s20072015. Article e2015.